Global Journal of Research in Engineering - Section A
GJRE

The use of Electromagnetic Suspensions in Improving the Dosing Efficiency of Powders

Eugeniu Ungureanu [§ * iD] and Pavel Topală [§ ‡ iD]

Affiliations
§ National University of Science and Technology POLITEHNICA Bucharest, Bucharest, Romania
‡ Alecu Russo State University of Bălți, Bălți, Republic of Moldova [(OA)]

Abstract

Localized powder feeding requires a controllable flow even for fine or agglomeration-prone materials. This paper presents a vibratory feeder in which magnetic granules are excited by an alternating electromagnetic field and agitate powder near the feeding path. The study reports operating observations across magnetic-granule counts, experimental flow-rate curves versus magnetic induction for WC, Al_2O_3, TiN, and Bro-10, and ten gravimetric measurements for each of six powder materials in a separate repeatability series at one fixed magnetic-field setting and 50 Hz. The six-material results are summarized by their arithmetic mean, sample standard deviation, and coefficient of variation. The measurements characterize prototype operation and repeatability; they do not establish absolute dosing error or a validated theoretical flow law.

Keywords: *electromagnetic actuation, localized powder delivery, magnetic granules, powder dosing, powder flow, vibratory feeder*

* **Corresponding Author**
Eugeniu Ungureanu, e-mail: ungureanusp5@gmail.com (primary contact), eugeniu.ungureanu@stud.fiir.upb.ro;
Pavel Topală, e-mail: pavel.topala@gmail.com

DOI
10.34257/GJREA278188

EARLY VIEW

1. Introduction

Metal and non-metal powders are used in additive manufacturing, powder metallurgy, coating deposition, assisted sintering, and electro-discharge processes. In these applications, a feeder does more than transport material from a reservoir. It must generate a controllable flow and introduce powder into the working zone without large variations in flow rate.

Powder flow is determined by particle size and shape, particle-size distribution, bulk density, roughness, moisture, electrostatic charge, and interparticle cohesion [1, 2]. Consequently, the same outlet geometry can produce different flow rates for different materials. The characterization of metal powders confirms that static and dynamic flow indicators must be interpreted together rather than separately [2].

At low flow rates, reducing the outlet opening promotes stable arch formation, local compaction, and intermittent discharge. Vibration can alter the network of contacts between particles, limit agglomeration, and mobilize material near the opening [3, 4, 5, 6, 7]. However, this effect is not universal; it depends on amplitude, frequency, fill level, geometry, and powder properties.

An earlier study examined powder-dosing systems and the limitations of existing feeders. The present work describes an original electromagnetic feeder and presents a preliminary experimental evaluation. The reported tests examine operating behavior as a function of magnetic-granule count, powder-flow response to magnetic induction, and repeated gravimetric measurements for selected powders. Further validation across calibrated clearance settings, reservoir fill levels, and actuator thermal conditions remains necessary before the results can be generalized.

1.1. Literature Review

The literature confirms that microdosing cannot be separated from powder properties. Fathollahi et al. showed that changes in effective density during feeding alter the flow rate and require material-specific calibration [8]. Later studies demonstrated that the control strategy must account for both material properties and process disturbances [9]. For cohesive powders, Hou et al. achieved continuous low-rate feeding by means of a dedicated design and reduced flow-rate variation [10].

For additive manufacturing, vibratory feeders offer the advantages of low inertia and rapid response to changes in the control signal. Sinclair et al. correlated flow rate with feeder parameters and the properties of metal powders [4]. Rothfelder et al. used vibratory microfeeding for localized delivery of metal and polymer powders [5]. Breese et al. emphasized that the flow supplied by a vibratory feeder can vary and that real-time monitoring is necessary when the process requires high repeatability [11].

Recent results reinforce this conclusion. Pasha et al. showed that ultrasonic vibration intensity, the initial amount of powder in the hopper, and the interaction between these variables significantly influence the powder dispensing rate [12]. Sanders et al. found in 2026 that active mechanical stirring can improve the consistency of cohesive-powder discharge [13]. These findings justify separating geometric adjustment from dynamic activation in the proposed device.

1.2. Functional Requirements

The requirements were formulated from the localized-feeding function and the failure modes encountered with fine powders.

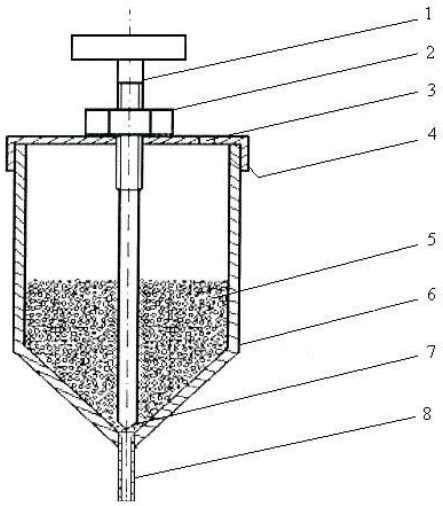
Table 1. Functional requirements of the vibratory feeder

Functional requirement	Adopted solution	Intended effect
Flow-rate adjustment	Axially adjustable cone forming an annular gap	Continuous change in cross-section without replacing the outlet
Flow activation	Ferromagnetic balls excited by an electromagnetic field beneath the conical plug	Break-up of powder agglomerates and local suspension formation
Localized discharge	Central lower outlet and coaxial geometry	Guiding the powder to a restricted processing zone
Geometric repeatability	Parametric CAD model, tolerances, and standardized fasteners	Maintaining the relative positions of the components
Maintainability	Removable covers, fittings, gasket, and electromagnet	Cleaning, inspection, and powder replacement
Low mass	Main components made of aluminum alloy	Efficient transmission of vibration

The device must permit continuous adjustment of the outlet cross-section, transmit vibration without significant parasitic deformation, maintain the coaxiality of the active components, and be removable for cleaning. Table 1 summarizes the adopted design responses and their intended effects.

1.3. Design and Operating Principle

For contact electro-discharge deposition of metal powders, the Elitron-22 installation used a conventional feeder mounted on the vibrating tool electrode holder. The metal-powder channel was adjusted by raising or lowering a dosing needle, which formed a gap between the needle and the hopper body (Figure 1). Approximately 20 g of metal powder were placed in the hopper while the dosing nozzle was closed. After the adjustment screw had been set to a minimum flow rate in the vibrator operating mode, the discharge time was measured and the powder collected through the nozzle was weighed using an analytical balance with 0.0001 g resolution. Once the required flow rate (g/min) had been established, dosing screw 1 was locked with nut 2 so that vibration could not alter the powder flow through the gap.

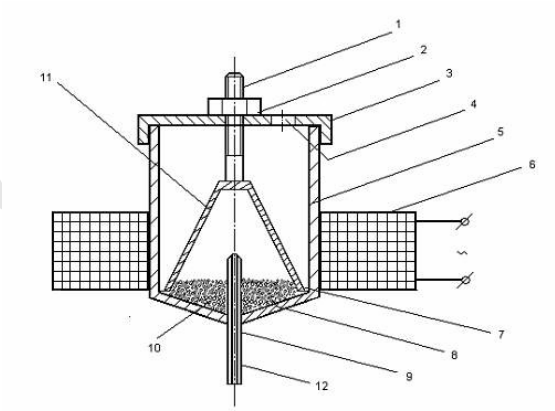


1, dosing screw; 2, locking nut; 3, feed opening; 4, hopper cover; 5, metal-powder granules; 6, hopper; 7, clearance ΔS between the hopper body and the dosing screw; 8, powder outlet nozzle.

Figure 1. Powder dosing device of the Elitron-22 installation.

The systems used in the Razread-M installation, like those described above, have several disadvantages. Adjusting the powder flow rate from the hopper requires the installation to be disconnected in order to raise or lower the dosing needle. In addition, powder flow can be interrupted by particle agglomeration at the outlet, a frequent occurrence when powders contain non-spherical particles.

In the design described in [23, 24, 25], the powder flow rate is adjusted without stopping the installation by changing the current intensity (Figure 2).



1, dosing screw; 2, locking nut; 3, hopper cover; 4, feed opening; 5, body; 6, electromagnetic coil; 7, clearance between body and hopper; 8, hopper; 9, powder discharge opening; 10, magnetized granules; 11, reservoir; 12, suspension outlet nozzle [26].

Figure 2. Powder dosing device of the Razread-M installation.

The device operates by forming a powder suspension inside the feeder. When coil 6 is connected to an alternating-current source, the magnetic field causes the granules to oscillate. Powder enters the feeder through the annular clearance formed by the threaded conical plug and the surrounding body. The axial position of the cone is adjusted by screwing or unscrewing it. The nominal geometric range stated for this clearance is 1.5d–0.8D, where d is the powder-particle diameter and D is the magnetic-granule diameter. The clearance limits are set to allow powder to enter from the reservoir while preventing magnetic granules from entering the powder-feed space. The powder-particle and magnetic-granule dimensions were known during the measurements. The clearance was set with screw 1 by bringing components 8 and 11 into contact and then turning the screw in the reverse direction to obtain the calculated clearance. The numerical value of the actual clearance was not measured. During each measurement series, the cone was fixed at one axial position and held constant.

2. Simplified Dynamic Model

The actual assembly is a distributed, nonlinear mechanical system. For a preliminary structural analysis, it was represented as a single-degree-of-freedom system [15, 16]. The equivalent mass m_e includes the body, covers, cone, and components that move together. The equivalent stiffness is k_e, while total damping c_e includes structural losses. Interaction between the field, magnetic balls, and powder additionally introduces apparent mass, impacts,

and variable damping. In Equation (1), F_0 is the equivalent force amplitude, $\omega = 2\pi f$ is the excitation angular frequency in rad/s, and c_e is an equivalent viscous damping coefficient in N · s/m. In the initial approximation, electromagnetic excitation is represented by an equivalent harmonic force:

$$m_e\ddot{x} + c_e\dot{x} + k_e x = F_0 \sin(\omega t) \tag{1}$$

The undamped natural angular frequency and the frequency expressed in hertz are:

$$\omega_n = \sqrt{\frac{k_e}{m_e}}, \qquad f_n = \frac{\omega_n}{2\pi} \tag{2}$$

For the steady harmonic regime, displacement amplitude can be written as:

$$X = \frac{F_0/k_e}{\sqrt{(1-r^2)^2 + (2\zeta r)^2}} \tag{3}$$

where the frequency ratio and damping factor are:

$$r = \frac{\omega}{\omega_n}, \qquad \zeta = \frac{c_e}{2\sqrt{k_e m_e}} \tag{4}$$

The model explains why the excitation frequency cannot be chosen independently of the mass and stiffness of the assembly. Approaching resonance can produce large amplitudes but may increase sensitivity to the amount of powder, screw tightening, and damping. Therefore, the stable operating regime must be established experimentally, not by calculation alone.

The powder and magnetic balls introduce nonlinear effects through impact, sliding, rotation, and contact reorganization. The response can change as the reservoir level decreases or when the number of balls changes. Studies of silos and vibratory conveyors show that vibration can either intensify or reduce flow depending on the dynamic regime and geometry [6, 7]. In the single-degree-of-freedom model, X is the structural displacement of the assembled feeder. Because the cone and body are treated as moving together, X does not directly modulate the cone-to-body clearance. The proposed effect on powder flow is indirect: motion of the assembly changes the motion and contact dynamics of the magnetic granules, whose impacts can transfer momentum to powder particles and alter their mobility and discharge. No quantitative relationship between X and P was measured in the present study.

3. Experimental Validation and Results

A design review confirmed that the documentation defines the parts, materials, tolerances, fasteners, and actuator integration. This check demonstrates the feasibility of manufacture and assembly, but it does not replace flow-rate validation. In the experimental series reported here, mass flow rate was determined gravimetrically:

$$P_i = \frac{m_{1i} - m_{0i}}{t} \tag{5}$$

where m_{0i} is the mass of the collection vessel before collection, m_{1i} is its mass after collection, and t is the dosing time. For $t = 1$ min, the mass difference in grams is numerically equal to the flow rate in g/min. The Bro-10 magnetic-induction sweep comprised ten repetitions at each reported B level. The six-material repeatability series comprised ten measurements per powder at one fixed B setting and 50 Hz; the same 60 s dosing duration was used. Data processing included the mean, sample standard deviation, and coefficient of variation.

The gravimetric method is suitable for prototype verification because it directly measures discharged mass. In recent literature, weighing is used both for the calibration of microfeeders and for the development of control strategies [8, 9, 11]. ISO 4490 may additionally be used to comparatively characterize the flow of metal powders through a calibrated funnel [22].

The experimental program comprised: (i) tests of feeder behavior and flow rate as a function of magnetic-granule count (Table 2); (ii) an experimental Bro-10 flow-rate sweep over several magnetic-induction levels (Figure 3); and (iii) ten gravimetric measurements for each of six powder materials at one fixed magnetic-induction setting (Table 3). Frequency was 50 Hz and each gravimetric measurement lasted 60 s. The conical plug position was held constant within each series. Clearance, reservoir fill level, and actuator thermal stability were not systematically varied.

3.1. Effect of the Number of Magnetic Granules on Feeder Powder Flow

The magnetic granules used as agitation bodies in the feeder are made of $BrFe_6$ and are spherical. In the absence of an external magnetic field, they can agglomerate and form clusters. It is therefore necessary to determine the number of granules for stable operation. In the electromagnetic field, they perform translational oscillatory motion at the field frequency (50 Hz); at the limit points, they rotate and align their magnetic poles with the applied field lines. The granule diameter was 2.68 mm. The number of magnetic granules loaded into the feeder was established by counting. For Table 2, "continuous" means that no interruption of discharge was observed during the run; "intermittent" means that at least one interruption was observed. The measurement and observation results are presented in Table 2.

Powder flow was classified as continuous or intermittent (with interruptions) based on the trace left on a strip of paper as the operating feeder was moved. In the recorded tests, 15–40 magnetic granules produced uninterrupted discharge in the low-count range. Continuous discharge was also observed at several larger counts, while intermittent discharge occurred in other count ranges. The results therefore do not establish a single continuous operating range or a monotonic threshold based on granule count alone.

3.2. Effect of Magnetic Induction B on Feeder Powder Flow

The Bro-10 series was used to determine the experimental dependence of powder flow rate on magnetic induction B. The tested magnetic-induction levels were 9, 10, 12, 15, and 18 mT at a supply frequency of 50 Hz. The protocol reported ten 60 s determinations per level; the Figure 3 curve represents the retained experimental results, and individual raw readings are not reproduced here.

Figure 3 presents the four experimental curves for tungsten carbide (WC), aluminum oxide (Al_2O_3), titanium nitride (TiN), and bronze (Bro-10), with particle diameters of 63–100 μm. The curves were digitized from the original graphical plot and redrawn with corrected axes and a key. They are used for qualitative comparison; the plotted point coordinates should not be treated as a substitute for the missing primary measurement records.

Across the plotted range, the experimental curves show an increase in flow with magnetic induction for each displayed material. This observation is limited to the tested setup and does not establish a universal material-independent power law.

3.3. Repeatability of the Six-Powder Measurements

For each of the six powder materials in Table 3, ten individual mass-flow measurements were made at one fixed magnetic-induction

EARLY VIEW

Table 2. Feeder operating behavior and powder flow rate as a function of the number of magnetic granules

No.	Number of granules	Flow rate [g/min]	Operating behavior	Number of granules	Flow rate [g/min]	Operating behavior
1	5	–	Continuous	120	0.0240	Continuous
2	10	–	Continuous	130	0.0256	Intermittent
3	15	0.0026	Continuous	140	0.0310	Intermittent
4	20	0.0142	Continuous	150	0.0390	Intermittent
5	25	0.0227	Continuous	160	0.0467	Intermittent
6	30	0.0436	Continuous	170	0.0508	Intermittent
7	35	0.0252	Continuous	180	0.0612	Intermittent
8	40	0.0274	Continuous	200	0.0624	Continuous
9	45	0.0179	Intermittent	250	0.0625	Continuous
10	50	0.0195	Intermittent	300	0.0650	Continuous
11	55	0.0209	Intermittent	350	0.0676	Continuous
12	60	0.0200	Intermittent	400	0.0841	Continuous
13	65	0.0191	Intermittent	420	0.0844	Continuous
14	70	0.0210	Intermittent	450	0.0846	Continuous
15	75	0.0211	Continuous	460	0.0850	Continuous
16	80	0.0320	Continuous	480	0.0874	Intermittent
17	90	0.218	Continuous	500	0.0878	Intermittent
18	100	0.0220	Continuous	550	0.0950	Intermittent
19	110	0.0224	Continuous	580	0.0918	Intermittent

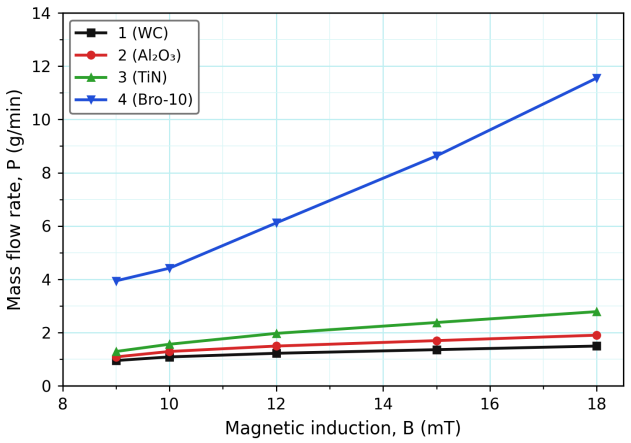


Figure 3. Experimental mass flow rate P versus magnetic induction B at 50 Hz, digitized from the original graph for replotting: (1) WC; (2) Al_2O_3; (3) TiN; (4) Bro-10. The curves are for qualitative comparison because tabulated coordinates were unavailable.

setting, 50 Hz, and a 60 s dosing duration. The arithmetic mean was calculated using Equation (6). The sample standard deviation and coefficient of variation were calculated from the same ten values. Because no independent target flow rate or reference value was specified, these statistics describe repeatability and are not an estimate of absolute dosing error.

$$\overline{P} = \frac{\sum_{i=1}^{n} P_i}{n} \tag{6}$$

For the six-material series, $n = 10$. The sample standard deviation was calculated as $s = \sqrt{\frac{\sum_{i=1}^{n}(P_i - \overline{P})^2}{n-1}}$, and the coefficient of variation as $\mathrm{CV} = \frac{100s}{\overline{P}}$.

The proposed solution differs from a simple vibrated hopper because it includes an active geometric adjustment element. The cone establishes the available cross-section, while the electromagnet modifies the dynamic state of the powder. The device can change from one operating regime to another without changing the outlet opening or dismantling the reservoir.

The design novelty results from integrating the following elements into a compact assembly: a cylindrical-conical chamber, an axially adjustable annular gap, localized central discharge, a mobile layer of magnetic balls placed beneath the conical plug, and an electromagnetic actuator separated from the powder path. The balls transform field variation into local volumetric agitation, not merely wall vibration. The design documentation enables reproducible, controlled modification of the geometry.

The solution also has limitations. Cone position cannot be directly converted into flow rate without calibration. Wear and deposits can alter the effective gap. Transmitted vibration depends on the assembly, powder level, and material properties. Research from 2025 and 2026 shows that the initial hopper mass and the form of mechanical activation must be treated as experimental variables rather than secondary conditions [12, 13].

At a later stage, a scale for cone position, a displacement sensor, and a feedback controller may be integrated. Closed-loop control is justified when the technological process requires automatic flow-rate maintenance [9, 11]. These developments should follow characterization of the basic device.

Table 3. Ten gravimetric flow-rate measurements and repeatability statistics for six powder materials

No.	TiC [g/min]	HfO_2 [g/min]	WC [g/min]	$Al_2O_3 + TiO_2$ (60:40) [g/min]	B_4C [g/min]	Mo [g/min]
1	0.0478	0.0836	0.0745	0.02908	3.540	0.0814
2	0.0480	0.0858	0.0738	0.02906	3.5414	0.0819
3	0.0492	0.0826	0.0742	0.02906	3.5421	0.0820
4	0.0483	0.0839	0.0745	0.02907	3.5418	0.0819
5	0.0497	0.0850	0.0744	0.02907	3.5427	0.0823
6	0.0480	0.0854	0.0741	0.02908	3.5421	0.0818
7	0.0488	0.0855	0.0743	0.02907	3.5418	0.0819
8	0.0489	0.0850	0.0740	0.02906	3.5423	0.0823
9	0.0490	0.0856	0.0739	0.02908	3.5427	0.0820
10	0.0470	0.0855	0.0742	0.02907	3.5421	0.0821
Mean, $\overline{P}$	0.04847	0.08479	0.07419	0.02907	3.54190	0.08196
Sample SD, s	0.00080	0.00106	0.00024	0.00001	0.00078	0.00026
CV (%)	1.642	1.252	0.327	0.028	0.022	0.316

Conditions for Table 3: one fixed magnetic-induction setting $B_0 = 12$ mT; supply frequency 50 Hz; dosing duration 60 s; $n = 10$ per material. The threaded cone was adjusted axially and held at the same setting for all repetitions. The nominal clearance range is 1.5d–0.8D; the numerical value of the actual clearance was not measured.

4. Conclusions

The design description and experimental results support the following conclusions:

- The feeder combines an axially adjustable conical clearance with electromagnetic agitation by magnetic granules.
- The simplified single-degree-of-freedom model describes structural response; it does not directly predict powder flow or clearance modulation.
- The Bro-10 measurements show an experimental change in flow rate across the tested magnetic-induction levels at 50 Hz.
- For six powder materials tested at one fixed magnetic-induction setting, ten repeated gravimetric measurements were summarized by mean, sample standard deviation, and coefficient of variation.
- The present results characterize prototype operation and repeatability. Because the numerical value of the clearance was not measured, absolute dosing accuracy cannot be assessed; generalization to other process conditions requires further validation under calibrated clearance settings.

REFERENCES

[1] Jaeger, H. M., & Nagel, S. R. Granular solids, liquids, and gases. Reviews of Modern Physics, 68, 1996, 1259–1273.

[2] Zegzulka, J., Gelnar, D., Jezerska, L., Prokes, R., & Rozbroj, J. Characterization and flowability methods for metal powders. Scientific Reports, 10, 2020, 21004. https://doi.org/10.1038/s41598-020-77974-3.

[3] Dunst, P., Bornmann, P., Hemsel, T., & Sextro, W. Vibration-assisted handling of dry fine powders. Actuators, 7(2), 2018, 18. https://doi.org/10.3390/act7020018.

[4] Sinclair, C. W., Edinger, R., Sparling, W., Molavi-Kakhki, A., & Labrecque, C. Vibratory powder feeding for powder bed additive manufacturing using water- and gas-atomized metal powders. Materials, 14(13), 2021, 3548. https://doi.org/10.3390/ma14133548.

[5] Rothfelder, R., Lanzl, L., Selzam, J., Drummer, D., & Schmidt, M. Vibrational microfeeding of polymer and metal powders for locally graded properties in powder-based additive manufacturing. Journal of Materials Engineering and Performance, 30, 2021, 8798–8809. https://doi.org/10.1007/s11665-021-06271-5.

[6] Hartig, J., Shetty, A., Conklin, D. R., & Weimer, A. W. Aeration and cohesive effects on flowability in a vibrating powder conveyor. Powder Technology, 408, 2022, 117724. https://doi.org/10.1016/j.powtec.2022.117724.

[7] Pascot, A., Morel, J.-Y., Antonyuk, S., Jenny, M., Cheny, Y., & Kiesgen De Richter, S. Discharge of vibrated granular silo: A grain-scale approach. Powder Technology, 397, 2022, 116998. https://doi.org/10.1016/j.powtec.2021.11.042.

[8] Fathollahi, S., Sacher, S., Escotet-Espinoza, M. S., DiNunzio, J., & Khinast, J. G. Performance evaluation of a high-precision low-dose powder feeder. AAPS PharmSciTech, 21, 2020, 301. https://doi.org/10.1208/s12249-020-01835-5.

[9] Fathollahi, S., Kruisz, J., Sacher, S., Rehrl, J., Escotet-Espinoza, M. S., DiNunzio, J., Glasser, B. J., & Khinast, J. G. Development of a controlled continuous low-dose feeding process. AAPS PharmSciTech, 22, 2021, 247. https://doi.org/10.1208/s12249-021-02104-9.

[10] Hou, P., Su, F., Pickering, L., Hickey, A., & Denyer, J. A continuous micro-feeder for cohesive pharmaceutical powders. International Journal of Pharmaceutics, 655, 2024, 123563. https://doi.org/10.1016/j.ijpharm.2024.123563.

[11] Breese, P. P., Hauser, T., Regulin, D., Seebauer, S., & Rupprecht, C. In situ measurement and closed-loop control for powder supply processes. The International Journal of Advanced Manufacturing Technology, 116, 2021, 889–903. https://doi.org/10.1007/s00170-021-07438-z.

[12] Pasha, M. M., Pei, Z., Kao, Y.-T., & Dubovick, K. Effects of ultrasonic vibration intensity and initial powder amount in the hopper on powder dispensing rate in binder jetting additive manufacturing. Journal of Manufacturing and Materials Processing, 9(8), 2025, 268. https://doi.org/10.3390/jmmp9080268.

EARLY VIEW

[13] Sanders, J., Kazi, S., Pei, Z. J., Kao, Y.-T., & Dubovick, K. Effects of auto-stirring on powder dispensing rate consistency in hopper-based binder jetting 3D printing with cohesive powder. Powders, 5(2), 2026, 21. https://doi.org/10.3390/powders5020021.

[14] Kharitonov, Y. S., Vasilyev, P., Bebikhov, Y. V., Egorov, A., & Semenov, A. Justifying the actuator type selection for the flow-line conveyor system with vibration-assisted transportation of bulk material. Transportation Research Procedia, 63, 2022, 2670–2677. https://doi.org/10.1016/j.trpro.2022.06.308.

[15] Rao, S. S. Mechanical Vibrations (6th ed.). Pearson, 2017.

[16] Inman, D. J. Engineering Vibration (4th ed.). Pearson, 2020.

[17] Rusin, E. P., Stazhevsky, S. B., & Khan, G. N. High-precision volumetric powder feeder. Journal of Applied Mechanics and Technical Physics, 2022. https://doi.org/10.1134/S0021894422030178.

[18] ASM International. Properties and Selection: Nonferrous Alloys and Special-Purpose Materials. ASM Handbook, Vol. 2. ASM International, 2020.

[19] ISO 965-1. ISO general purpose metric screw threads—Tolerances—Part 1: Principles and basic data.

[20] ISO 2768-1. General tolerances—Part 1: Tolerances for linear and angular dimensions without individual tolerance indications.

[21] ISO 4762. Hexagon socket head cap screws.

[22] ISO 4490:2018. Metallic powders—Determination of flow rate by means of a calibrated funnel (Hall flowmeter).

[23] Gitlevich, A. E., Topala, P. A., & Kuku, I. I. Device for Supplying Powder Material. USSR Author's Certificate No. 1574385, B23H 9/00; application No. 4380835/31-08, 22 February 1988; Bulletin of Inventions, 1989, No. 24, 2 pp.

[24] Topală, P. Powder Dosing Device. Specialized International Exhibition Moldexpo, Official Catalog, Chisinau, 1999, p. 55.

[25] Topală, P. Powder Dosing Device. Inventa 1999: 5th International Salon of Technical Innovations, Bucharest, 26–29 May 1999, p. 90. Presentation of USSR Author's Certificate No. 1574385.

[26] Nemoshkalenko, V. V., Topala, P. A., Tomashevsky, N. A., Mazanko, V. F., & Nosovsky, O. I. Specific features of surface-layer formation during spark discharges. Metallofizika, 12(3), 1990, pp. 132–133.

EARLY VIEW